Preferred citation: C.K. Meadley. High-speed filtration of compressible fibrous media. In **Consolidation of the Paper Web**, *Trans. of the IIIrd Fund. Res. Symp. Cambridge, 1965*, (F. Bolam, ed.), pp 216–238, FRC, Manchester, 2018. DOI: 10.15376/frc.1965.1.216.

HIGH-SPEED FILTRATION OF COMPRESSIBLE FIBROUS MEDIA

C. K. MEADLEY, Joseph Dixon Research Fellow, Faculty of Technology, University of Manchester

Synopsis—Experiments with synthetic fibres and a special flow apparatus, yielding data for the water permeation of fibre mats in the viscous-turbulent flow regime are briefly described. It is found that, within the range of the variables concerned, the results conform well to a recently established empirical equation relating the flow resistance of a pad to the flow speed, pad porosity and fibre specific surface. This empirical expression is then used, along with an equation representing wet mat compression characteristics, to construct a theoretical model of high-speed filtration. The result is a system of non-linear partial differential equations for the suspension kinematics and the flow rate/density distributions within the forming mat. Examples of numerical solutions are presented and discussed.

When a constant pressure is applied to a fibre slurry initially at rest, it undergoes a continuously decreasing acceleration, reaching a maximum filtration speed, after which the speed decreases uniformly, corresponding to a constant pressure drop filtration process. The peak speed may be as much as eight times greater than the speed characterising the final constant pressure zone. Theoretical results for the density distribution in a forming mat illustrate the effect of relative compressibility, for which the more compressible material exhibits a rapidly changing density profile near the supporting septum. It is also found that the rate at which the mat builds up after peak slurry speed decreases with increasing time to an extent depending on the mat compressibility. Filtration experiments with a bleached sulphite pulp yield results that agree satisfactorily with the calculations, confirming predicted formation times to within less than 10 per cent. The experiments thus further corroborate the predicted inverse relationship of formation time with applied pressure, as well as an approximate proportionality of formation time and sheet substance.

Nomenclature

g = acceleration of gravity
h_0 = total depth of fibre suspension above septum before filtration
h = depth of fibre suspension above septum during filtration

k = Kozeny factor, considered as an empirical function of porosity
L = thickness of fibre mat or porous medium
m, n = empirical constants characterising fibre mat compressibility
p = static pressure of the fluid phase
p_A = static pressure at the filtrate free surface
p_0 = static pressure at the suspension free surface
Δp_A = applied pressure, defined by $(p_0 - p_A)$
Δp = pressure drop across the fibre mat
R = dimensionless fluid flow rate—or Reynolds Number—defined by $\rho V/\mu S_0$ and calculated at points within the fibre mat
R_e = permeation Reynolds Number for fibre mats defined by $\rho V/\mu S_0(1-\epsilon)k^{1/2}$
R_0 = dimensionless flow rate of the fibre suspension defined by $\rho V_0/\mu S_0$
S_0 = wet specific surface area of the filtered particles, area per unit volume of solids
t = time
t' = non-dimensional time, defined by $(\theta^n \mu^3 S_0{}^4/mn\rho^2)t$
V = fluid permeation velocity, defined at a point as the ratio of the volumetric flow to the enclosing sectional area normal to the mean flow direction
V_0 = fibre suspension velocity, incident to the mat face
θ = wet specific volume of the filtered particles; wet volume per unit oven-dry mass
x = space co-ordinate, specifying a point within the fibre mat as distance from the supporting septum
x' = non-dimensional space co-ordinate, defined by $(\theta^n \mu^2 S_0{}^3/mn\rho)x$
α = non-dimensional constant defined by $\theta^{2n} h_0 \mu^4 S_0{}^5/m^2 n\rho^2$
β = non-dimensional constant defined by $\rho_S \theta$
γ = non-dimensional constant defined by $(\theta^n/m)(\Delta p_A + h_0 \rho g)$
ϵ = porosity of fibre mat or porous medium; three-dimensional void fraction
η = non-dimensional mat thickness, defined by $(\theta^n \mu^2 S_0{}^3/mn\rho)L$
μ = viscosity of fluid phase
ξ = relative mat depth defined by $(\eta - x')/\eta$
ρ = density of fluid phase
ρ_S = consistency of fibre suspension; dry mass of dispersed fibres per unit volume of the suspension
ρ_B = bulk density of deposited fibre mat; dry mass of fibres per unit spatial volume
ψ = three-dimensional solidity of the fibre mat, defined by $(1-\epsilon)$ and given by $\theta \rho_B$

Introduction

THE PROCESS of filtration may be broadly defined as the controlled separation of solid particles from a suspension in a fluid phase. The separation is usually effected by forcing the suspension through a medium that is permeable to the fluid, but impermeable to the solid. As the particles are removed from the suspending fluid, they collect on the separating medium or septum, which generally is a rectangular grid of high porosity. Here, they form an ever-increasing thickness of porous cake or mat, through which the fluid must permeate. Depending on the relative compressibility of the network of filtered particles, a density field may be established within the forming mat as a consequence of the fluid drag forces inherent in the permeation process. It may be inferred, therefore, that any study of the nature of filtration requires a prior knowledge of the filtered medium compressibility characteristics and in particular the laws of permeation relating to the media concerned.

Permeation in general refers to the flow of a fluid through a uniform sample of an incompressible porous medium. When the sample is composed of an unconsolidated system of particles, such as fibres, it may be characterised by its uniform porosity ϵ and particle specific surface area S_0; the fluid, when incompressible, is characterised by its density ρ and viscosity μ. If the fluid is forced to flow at a superficial rate V through the porous medium, it suffers a pressure gradient dp/dL as a result of the frictional and turbulent shear stresses set up within the interstices. The study of permeation attempts to establish the relationship between these variables, which might be expressed by—

$$dp/dL = f(\epsilon, S_0, \mu, \rho, V) \quad . \quad . \quad . \quad (1)$$

The greatest proportion of knowledge about permeation concerns the viscous flow regime, for which the pressure gradient across a given porous medium varies in proportion to the flow rate. In this case, equation (*1*) has the form—

$$dp/dL = f_1(\epsilon, S_0, \mu, \rho)V \quad . \quad . \quad . \quad . \quad (2)$$

which is a generalised expression of the well-known Darcy's law. The form of the function f_1 has been the subject of extensive investigations, the most notable result being the frequently discussed Kozeny-Carman equation, which has been thoroughly reviewed.[1] It appears that universal formulation cannot be established and that the empirical expressions are to some extent dependent on particle shape and porosity range. It has been illustrated[2] that, because of inherent difficulties associated with the boundary conditions of porous media, exact theoretical calculation of permeation is very limited; thus, knowledge must remain highly dependent on the empirical correlation of experimental data.

Given the valid empirical expressions for the permeation and compression characteristics of a certain porous medium, however, it is possible to predict theoretically the nature of associated phenomena such as filtration. For the low-speed range of Darcy's law, filtration processes have been calculated,[3] showing the influence of compression and predicting a flow rate and porosity distribution throughout the forming mat. In the case of beds of fibrous particles, the relevant form of equation (*2*) has been used extensively for filtration applications in the paper industry.[4-6] An extended version of the Kozeny-Carman equation, applicable to filtered fibres and expressing more accurately the influence of porosity, has been carefully established[7] and has been used to calculate the filtration of compressible fibrous beds under the laminar flow conditions.[8]

When the permeation flow rate is large enough, visco-turbulent conditions will prevail, with the result that the laminar flow basis of Darcy's law breaks down, rendering all associated calculations inapplicable. In this case, the energy loss from permeation is a combination of viscous and turbulent stresses. Extensive study of permeation through granular material[9] has shown that the form of equation (*1*) suitable to represent data at high speeds is—

$$dp/dL = f_1(\epsilon, S_0, \mu, \rho)V + f_2(\epsilon, S_0, \mu, \rho)V^2 \qquad . \quad . \quad (3)$$

which reduces at low speeds to the form acceptable for viscous flow. The functions f_1 and f_2 can be established experimentally to represent a wide variety of particles, but evidence still suggests a dependence on general class or shape.

Recent experimental work on the high-speed permeation of water through fibre beds[10] has established the following relationship—

$$dp/dL = \left[\frac{\mu S_0{}^2(1-\epsilon)^2 k}{\epsilon^3}\right] V + \left[\frac{0.1(1-\epsilon)S_0 k^{1/2}\rho}{\epsilon^3}\right] V^2 \qquad . \quad (4)$$

where

$$k = \frac{3.5\epsilon^3}{(1-\epsilon)^{1/2}}\,[1+57(1-\epsilon)^3] \qquad . \quad . \quad . \quad (5)$$

The expressions given in this case for the functions f_1 and f_2 apply strictly to permeation of mats having fibres oriented randomly in planes normal to the direction of flow. This type of orientation is, however, characteristic of fibre beds deposited by filtration and therefore permits the use of equation (*4*) for filtration analysis.

Theoretical knowledge of high-speed filtration phenomena, of the kind which has been established for the viscous regime, appears to be seriously lacking, in particular for fibre suspensions. Although empirical data have been advanced on a semi-quantitative basis[11-13] to provide a broad experimental foundation for permeation and filtration of fibres, an understanding of the theoretical link between the two processes remains to be established for the visco-turbulent regime.

The objectives of the present investigation were as follows—

1. To establish experimentally an additional degree of confidence in the empirical expression that has been propounded to describe high-speed permeation of fibre beds—equation (*4*).
2. Accepting the formal character of equation (*4*), to deduce its consequences for high-speed filtration with the aid of a theoretical model of the process.
3. Partially to corroborate the predictions of the theory with high-speed filtration measurements on a bleached sulphite pulp.

Experimental

THE PRIMARY purpose of the experimental work was to investigate and reconfirm the validity of equation (*4*) to represent the high-speed permeation of fibre mats. In accord with the usual approach,[1, 10, 13] synthetic fibres of known and verified geometrical properties were used to test the correlation.

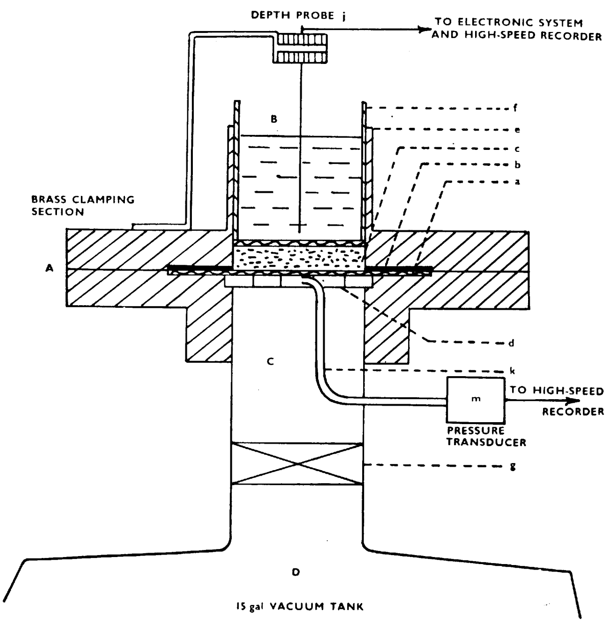

Fig. 1—Experimental apparatus

The wide range of fibre characteristics, as well as the particular experimental technique, provided a suitable variation of the conditions under which the correlation was originally evolved.[10]

The apparatus shown schematically in Fig. 1 was constructed to study both permeation and filtration. The design is similar in operating principle to that of machines used for previous filtration studies,[11-13] but incorporates slight modifications to meet more closely the demands of the present investigation. The apparatus consists of a cylindrical brass clamping section, which connects via a continuous smooth bore pipe through a quick-acting valve to a 15 gal vacuum tank. The brass portion A is composed of two parts hinged in such a way that, when clamped, they provide an airtight seal around the flow chamber *B–C*. A 6 in diameter wire mesh *a* (70/52 mesh, 21 per cent open area) is clamped beneath a rubber gasket *b* and exposes a 3 in diameter working section, upon which the fibre pad is deposited in position *c*. This wire mesh, which was used throughout the studies, is rigidly supported in the flow chamber by the flow eveners *d*. The fibre mat is formed by slow filtration of a very dilute suspension from a supplementary device fitted to the cylinder *e*. After formation, the mat is compressed from above by a second wire mesh fitted to the depressor *f*, which is clamped rigidly in place to maintain a known pad depth L and average porosity ϵ.

The permeating fluid is placed over the mat in chamber B and is supported in place by the air cushion in chamber C when the gate valve g is closed. After evacuation of the tank D to a desired level of vacuum, opening the valve then initiates permeation of the mat. The volume ratio D/C is such as to permit the optimum fast application of vacuum to the control fluid in chamber B. The motion of the fluid is measured by the depth probe j, which records the depth in time $h(t)$ by an electrical resistance principle. The pressure drop across the pad $\Delta p(t)$ is measured simultaneously by the sensing tube k and pressure transducer m, which record the static pressure directly under the supporting grid. For equilibrium flow conditions and making use of an accurate calibration of the depth probe, these recordings then provide corresponding values of the permeation rate V and pressure gradient $\Delta p/L$. Different magnitudes of V are produced by various settings of applied vacuum.

Results

Uniform, cylindrical, staple-length synthetic fibres made from Terylene and nylon were used for the permeation experiments. The deniers were chosen to represent a wide range of fibre size, having wet diameters of 16 μ (2 denier nylon), 26 μ (6 denier Terylene) and 49 μ (18 denier nylon), thus providing an experimental variation in specific surface area S_0 from 2 460 to 823 cm^{-1}, respectively. Series of tests were performed each at different pad basis weights ranging 0.046–0.15 g/cm^2 and at average pad porosities within 0.78–0.93. Water at temperatures of 12–20°C was used to permeate the fibre beds at speeds V up to 180 cm/sec.

According to the conventional approach,[9, 10] the measurements are most easily correlated by calculating the non-dimensional friction factor f and Reynolds Number R_e defined for fibres as—

$$\left.\begin{aligned} f &= \frac{\epsilon^3 \Delta p}{(1-\epsilon)S_0 k^{1/2} \rho L V^2} \\ R_e &= \frac{\rho V}{\mu S_0 (1-\epsilon) k^{1/2}} \end{aligned}\right| \quad . \quad . \quad . \quad (6)$$

where k is calculated from the porosity according to equation (*5*). The experimental values of f and R_e have been plotted for all test series and for each fibre size in Fig. 2. Using the definitions (*6*), equation (*4*) reduces to—

$$f = (R_e)^{-1} + 0.1 \quad . \quad . \quad . \quad . \quad (7)$$

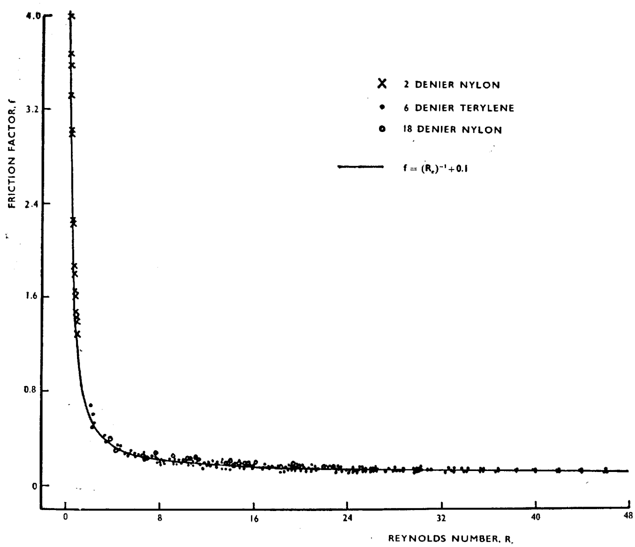

Fig. 2—Correlation of permeation data

This is the suggested correlation,[10] which is also graphed for comparison with the data. It is apparent from Fig. 2 that equation (*7*) is a satisfactory representation of the permeation measurements. For the wide range of experimental conditions and fibre characteristics used, the agreement is considered good and suggests that the form of equation (*4*) is an adequate empirical description of high-speed fibre permeation.

Theoretical treatment of high-speed filtration

Basic model

HAVING established experimentally some degree of confidence in the reliability of equation (*4*) to describe fibre mat permeation, it is of interest next to deduce the consequences of its formal character on the process of filtration. For this purpose, a theoretical model of filtration is used and is defined schematically in Fig. 3.

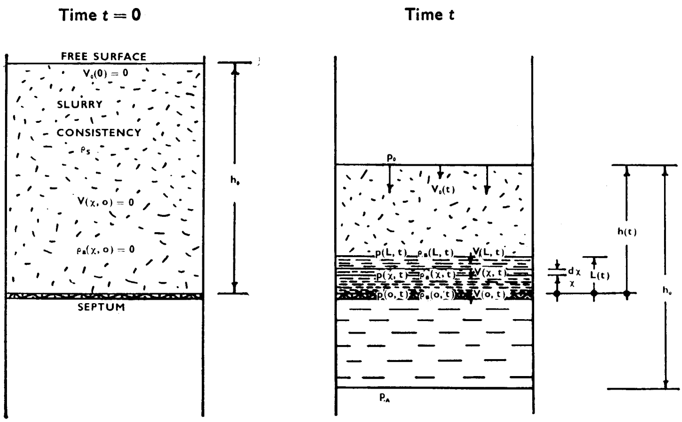

Fig. 3—Theoretical model of filtration

The model corresponds to a general class of filtration such as may be found in many practical forming devices and in particular in the experimental apparatus (Fig. 1). Initially, a uniform suspension of fibres at consistency ρ_S covers the wire mesh to a depth h_0. At time $t = 0$, a pressure drop $(p_0 - p_A)$ is applied across the suspension, causing it to accelerate from rest and form a continuously compressing mat such as sketched to represent any time t. No demands with regard to the type of process (for example, constant rate or constant pressure filtration) are made. The use of assumptions, both implicit and explicit, however, is necessary to remove many complicating secondary effects from the fundamental mechanics of the process, which is the primary consideration of the model.

Assumptions

1. The fibre suspension is uniform and isotropic; no granular or very fine particles are present.

2. The deposited fibre mat has a bulk density distribution, which is continuous in the direction of flow and invariant in directions normal to the flow.

3. The supporting wire mesh contributes negligible resistance to the flow.

4. At high rates of formation, the fibre motion within the deposited mat caused by compression is negligible.

5. Water retention within the mat has negligible influence on the flow rates.

6. The wire mesh and fibre length are of such a size that fibre retention is complete.

7. The fibre mat is conceived as a 'porous continuum', without regard to the contribution of individual fibres.

Assumptions (*1*) and (*2*) express the condition that there is no flocculation within either the mat or the suspension. Although flocculation may be of practical importance in some cases, analysis of such effects are not within the scope of the present theoretical objectives. Assumptions (*3*) and (*4*) refer to factors more easily treated mathematically, but which have been excluded for formal simplicity, similarly to previous calculations of viscous filtration.[3, 8] They represent refinements of the theory, which may be considered in some specific case with the object of improved accuracy. This has been done in the present study and the assumptions have been found to be justified to the order of $1 \sim 2$ per cent. Assumption (*5*), for which additional empirical information concerning water retention is necessary, has been similarly justified and assumption (*6*) excludes the additional highly complicating factor of through-flow, whose intrinsic effect is preferably investigated as a separate problem.

Fundamental relationships

Referring to Fig. 3 and using assumptions (*1*) and (*2*), it may be stated that for time-dependent flow conditions, the forming filter pad is characterised by a depth-time distribution of bulk density $\rho_B(x, t)$. This results from the fibre network compressibility and the fluid drag associated with permeation. The fluid motion may be characterised by a flow rate and pressure distribution denoted by $V(x, t)$ and $p(x, t)$, respectively. The object of the problem is to evaluate these functions and find the resultant kinematic behaviour of the suspension $V_0(t)$.

The reference frame is anchored in the stationary wire mesh such that the slurry level is specified by $h(t)$, with $h(0) = h_0$. The fibre mat thickness is denoted by $L(t)$, representing an unsteady bound for the space co-ordinate x, defined by the domain—

$$0 \leqslant x \leqslant L(t) \quad . \quad . \quad . \quad . \quad (8)$$

for which the functions $\rho_B(x, t)$, $V(x, t)$ and $p(x, t)$ are desired.

Permeability—Application of the visco-turbulent permeation relationship—equation (*4*)—at time t to the fibrous layer at point x, having infinitesimal thickness dx and through which the flow rate is $V(x, t)$ yields, in the limit as $dx \to 0$, the following—

$$\frac{\partial p}{\partial x} = \frac{\mu S_0{}^2(1-\epsilon)^2 k(\epsilon)}{\epsilon^3} |V(x, t)| + \frac{0.1(1-\epsilon)S_0 k^{1/2}(\epsilon)\rho}{\epsilon^3} V^2(x, t) \quad . \quad (9)$$

where the function $k(\epsilon)$ is given by equation (*5*).

Compressibility—Considerable experimental work has shown that, when a uniform fibrous layer is compacted by and in elastic equilibrium with an externally applied pressure, the resulting mat density may be related to the pressure by a simple power function. This fact has been used frequently[7, 8] with success for the formulation of compresson effects in flow problems; its consequence in the present case, when considering the layer of thickness dx, for which the density and elastic forces may be assumed uniform, is—

$$p(L, t) - p(x, t) = m[\rho_B(x, t)]^n \quad . \quad . \quad . \quad (10)$$

which specifies the continuous relationship for the limit as $dx \to 0$. Here, the parameters m and n are constants characterising the compressibility of the fibrous medium. They may be obtained, when desired, from laboratory experiments.[7]

Flow continuity—If the filtrate is an incompressible fluid and the mat is compressing, then the flow rate must vary within the mat as a consequence of the rate of change of void space. The conservation of fluid mass therefore requires that—

$$\frac{\partial}{\partial x} |V(x, t)| = \frac{\partial}{\partial t} \epsilon(x, t) \quad . \quad . \quad . \quad (11)$$

Conservation of fibre mass—This principle, which is an inherent aspect of the filtration process, expresses the fact that a balance of fibres must be maintained. In the absence of through-flow—assumption (*6*)—the sum of the masses of deposited fibres and the remaining dispersed fibres must equal the total mass initially suspended at time $t=0$. Consequently, with reference to Fig. 3, there results—

$$[h(t) - L(t)]\rho_S + \int_0^{L(t)} \rho_B(x, t)dx = \rho_S h_0$$

where integration is partial with respect to x. By definition—

$$h_0 - h = \int_0^t |V_0(t)| dt$$

and therefore— $$\int_0^{L(t)} \rho_B(x, t)dx = \rho_S \int_0^t |V_0(t)| dt + \rho_S L(t) \quad . \quad . \quad (12)$$

Conservation of momentum—The complete body of fluid defined by h_0 is controlled mechanically by the values of applied pressure and total mat resistance. Recalling assumptions (*3*) and (*5*), an inertial force balance yields—

$$\Delta p_A + \rho g h_0 - [p(L, t) - p(0, t)] = h_0 \rho \frac{d}{dt} |V_0(t)| \quad . \quad (13)$$

where $\Delta p_A = (p_0 - p_A)$ denotes the applied pressure.

Flow at the mat face—The formulation of boundary conditions at the mat face necessarily requires a consistent mathematical definition of this surface. In the case of filtration, it has formerly been considered[(8)] as the point at which the mat density equals that of the approaching slurry. It is difficult, however, to make this concept compatible with high-speed filtration of dilute suspensions or the permeation of an unconstrained compressible mat.[(7)] In each case, the mat formation at the surface ought to result from the same principle; it would seem therefore that fundamentally the surface structure is independent of the slurry consistency and is more probably specified by the entrance flow rate and the relevant permeability relationship.

The mat face may be defined simply as that point $x = L$ beyond which there is no fibre mass in a state of permeation and at which the hydrodynamic drag ceases to act. Therefore, as implied by equation (*10*), the requirement that—

$$\rho_B(L, t) = 0 \quad . \quad . \quad . \quad . \quad (14)$$

will be assumed here to be the rigorous definition of the pad surface. Matching the permeation rate at the surface with the slurry approach speed, in view of assumptions (*4*) and (*5*), results in—

$$V(L, t) = (1 - \rho_S \theta) V_0(t) \quad . \quad . \quad . \quad (15)$$

where θ, the fibre specific volume, is assumed constant and satisfies the relationship—

$$\epsilon(x, t) = 1 - \theta \rho_B(x, t) \quad . \quad . \quad . \quad (16)$$

Substitution of equations (*5*), (*10*) and (16) into equation (*9*) yields—

$$\frac{\partial \rho_B}{\partial x} = -\frac{\theta^{n-1}}{mn} \left[\frac{3.5 \mu S_0^2 [1 + 57(\theta \rho_B)^3]}{(\theta \rho_B)^{n-2.5}} |V| + \frac{0.187 S_0 \rho \sqrt{1 + 57(\theta \rho_B)^3}}{(1 - \theta \rho_B)^{3/2} (\theta \rho_B)^{n-1.75}} V^2 \right] \quad (17)$$

To express the notion that the surface must form in such a way that the relevant permeability relationship is satisfied for a finite entrance speed requires that conditions (*14*) and (*15*) are imposed on equation (*17*). The result is an infinite density gradient at the mat face, which when considered with condition (*14*) gives a reasonable physical concept.

The structure very close to the mat face, which will depend only on the approach flow rate and the compression/permeability relationships, may be investigated by taking the limit for very small density, $\rho_B \to 0$. This means formally that, in view of equation (*14*), the following obtains—

$$\lim_{x \to L} \{\rho_B(x, t)\} = 0$$

Solving equation (*17*) as a quadratic for $|V|$, in consideration of equation (*15*) produces—

$$\lim_{x \to L} \{|V(x, t)|\} = (1-\rho_S\theta)|V_0(t)| = \tfrac{1}{2}\left\{\frac{4mn\theta^{1-n}}{0.187S_0\rho}(\theta\rho_B)^{n-1.75}\left|\frac{\partial\rho_B}{\partial x}\right|\right\}^{1/2}$$

which may be integrated to yield—

$$\theta\rho_B(x, t) = \left[\frac{0.187\theta^n}{mn}(n-0.75)(1-\rho_S\theta)^2V_0^2(t)S_0\rho(L(t)-x)\right]^{1/(n-0.75)} \quad (18)$$

This result, giving the density distribution close to and at the pad surface, is the boundary condition that must be satisfied by the functions $V_0(t)$ and $\rho_B(x, t)$ in the limit as $x \to L$.

Initial condition—The suspension is initially at rest with no deposition of fibre.

Consequently,

$$\left.\begin{aligned} \rho_B(x, 0) &= 0 \\ V(x, 0) &= 0 \\ L(0) &= 0 \end{aligned}\right| \quad (19)$$

Transformation of equations

Introducing the non-dimensional variables—

$$\left.\begin{aligned} x' &= \frac{\theta^n\mu^2S_0^3}{mn\rho}x \\ t' &= \frac{\theta^n\mu^3S_0^4}{mn\rho^2}t \\ R &= \frac{\rho}{\mu S_0}V \\ \psi &= \theta\rho_B \\ \eta &= \frac{\theta^n\mu^2S_0^3}{mn\rho}L \end{aligned}\right| \quad (20)$$

and non-dimensional constants—

$$\left.\begin{aligned} \alpha &= \frac{\theta^{2n} h_0 \mu^4 S_0{}^5}{m^2 n \rho^2} \\ \beta &= \rho_S \theta \\ \gamma &= \frac{\theta^n}{m} (\Delta p_A + h_0 \rho g) \end{aligned}\right| \qquad (21)$$

and redefining the space co-ordinate as the relative mat depth, measured from the surface—

$$\xi = \frac{\eta - x'}{\eta} \qquad (22)$$

reduces equations (*10*) to (*19*) to the system—

$$\left.\begin{aligned} \frac{\partial \psi}{\partial \xi} &= \eta \left[\frac{3.5(1+57\psi^3)}{\psi^{n-2.5}} R + \frac{0.187\sqrt{1+57\psi^3}}{\psi^{n-1.75}(1-\psi)^{3/2}} R^2 \right] \\ \frac{\partial R}{\partial \xi} &= \eta \frac{\partial \psi}{\partial t'} + \frac{d\eta}{dt'} (1-\xi) \frac{\partial \psi}{\partial \xi} \\ \eta &= \frac{\eta}{\beta} \int_0^1 \psi d\xi - \int_0^{t'} R_0 \, dt' \\ R_0(t') &= R(0, t')/(1-\beta) \end{aligned}\right| \qquad (23)$$

having boundary conditions—

$$\left.\begin{aligned} \gamma - \psi^n(1, t') &= \alpha \frac{dR_0}{dt'} \\ \lim_{\xi \to 0} \{\psi(\xi, t')\} &= [0.187(n-0.75)(1-\beta)^2 R_0{}^2 \eta \xi]^{1/(n-0.75)} \end{aligned}\right| \qquad (24)$$

and initial conditions—

$$\left.\begin{aligned} \psi(\xi, 0) &= 0 \\ R(\xi, 0) &= 0 \\ \eta(0) &= 0 \end{aligned}\right| \qquad (25)$$

The system (*23*) is a set of four simultaneous equations to be solved for the four functions $\psi(\xi, t')$, $R(\xi, t')$, $\eta(t')$ and $R_0(t')$. Use of the non-dimensional variables (*20*) and constants (*21*) has reduced the nine physical parameters of the original equations to the minimum of four required for a solution. Upon examination, it is apparent that conditions (*24*) and (*25*) are sufficient to specify a unique solution for given values of α, β, γ and n, but the non-linear character of the partial differential equations is such that numerical methods are required for solution.

Results

A technique has been developed[14] that permits solution of equations (*23*)–(*25*) by direct numerical integration. With the aid of the Atlas digital computer of the University of Manchester, solutions have been prepared to cover the practical range of the parameters α, β, γ and n.

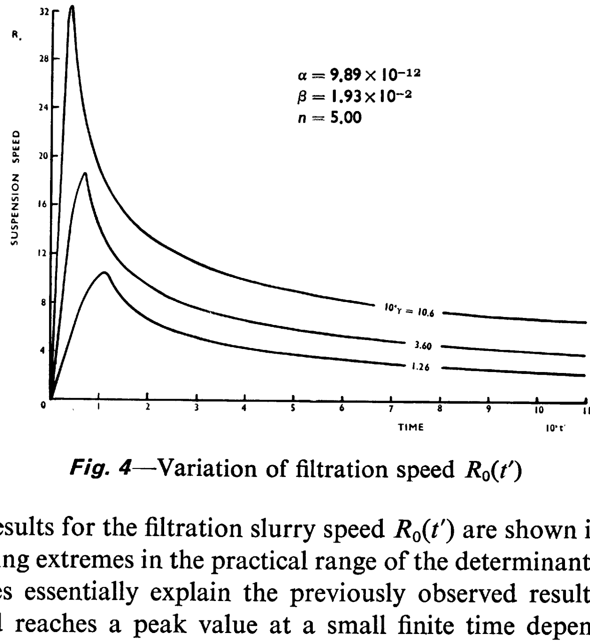

Fig. 4—Variation of filtration speed $R_0(t')$

Typical results for the filtration slurry speed $R_0(t')$ are shown in Fig. 4 and 5, representing extremes in the practical range of the determinant parameters. These curves essentially explain the previously observed result[11] that the slurry speed reaches a peak value at a small finite time depending on the imposed acceleration and media characteristics. The corresponding solutions for the static pressure $p(\xi, t')$, obtained with the aid of the relationship (*10*), show that the motion after peak speed represents constant pressure filtration, where the total pressure drop across the forming pad is in equilibrium with the applied pressure. Any given curve may be resolved into three practical zones—

1. Motion of the slurry under essentially uniform acceleration (depending on the value of γ).
2. Decreasing acceleration of the slurry as the forming mat resistance becomes significant.
3. After peak speed, motion of the slurry under constant pressure filtration.

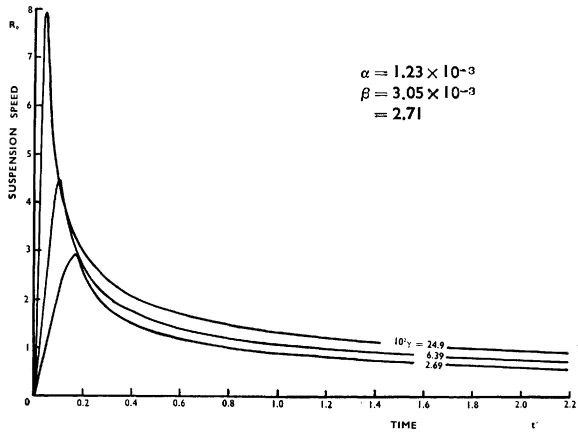

Fig. 5—Variation of filtration speed $R_0(t')$

Zones (*1*) and (*2*) will be referred to as initial formation and zone (*3*) as final or constant pressure formation.

The parametric values of Fig. 5, in comparison with those of Fig. 4, represent the more compressible, finer particle mats. It may be inferred therefore that, for the same relative change in applied pressure, the more compressible media exhibit the least difference in final filtration rates.

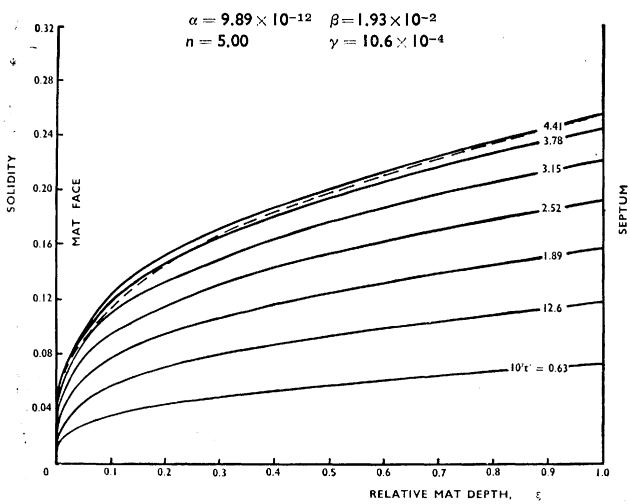

Fig. 6—Solidity profiles $\psi(\xi, t')$

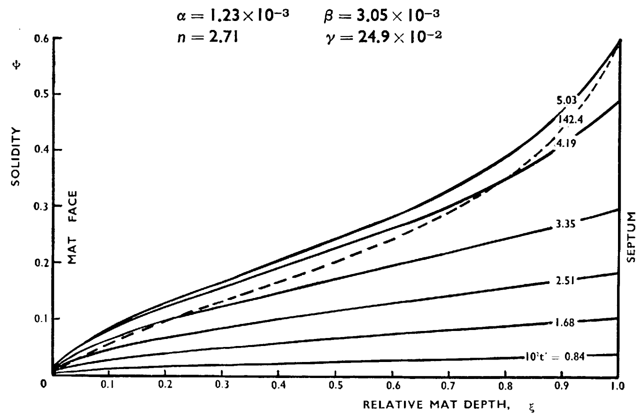

Fig. 7—Solidity profiles $\psi(\xi, t')$

For each parametric curve of $R_0(t')$, there corresponds a compression solidity distribution $\psi(\xi, t')$. Profiles of such distributions, corresponding to the highest γ values of Fig. 4 and 5, are shown in Fig. 6 and 7, respectively. Fig. 6 demonstrates the way in which solidity varies in a relatively incompressible mat during the initial formation period. The dotted curve represents $\psi(\xi)$ for large times, indicating that the relative nature of compression changes very little during constant pressure formation. The curves of Fig. 7

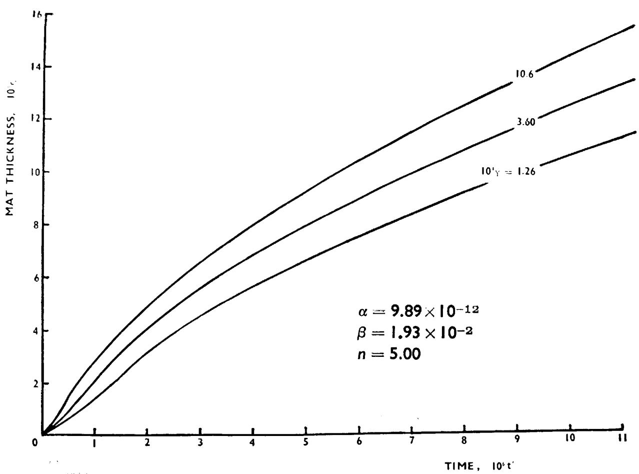

Fig. 8—Growth of filter mat $\eta(t')$

differ in character from those of Fig. 6 by having a distinct inflexion point; the effect of compressibility is clearly shown by the rapidly increasing solidity near the septum.

The nature of the mat formation is shown in Fig. 8 and corresponds to the parameters of Fig. 4. It is apparent that the mat growth during the acceleration period is intrinsically different from that of the constant pressure filtration. The latter is, however, more significant with respect to total behaviour and displays a decreasing growth rate with increasing time. Additional solutions for $\eta(t')$ have shown more pronounced, but similar effects for increased compressibility.

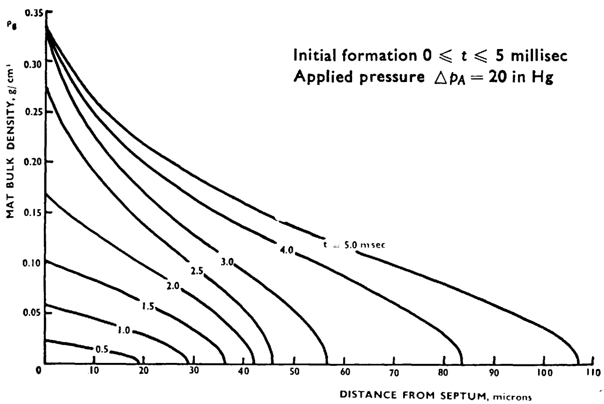

Fig. 9—Fibre mat density distribution $\rho_B(\chi, t)$—filtration of classified unbeaten sulphite fibres

The parametric values of Fig. 5 and 7 actually represent the physical and compression characteristics of a classified sulphite fibre mat that is filtered from a suspension depth of $h_0 = 6$ cm by the application of a vacuum $\Delta p_A =$ 20 in Hg to form a 100 g/m^2 sheet. Consequently, it is possible to make theoretical predictions of the high-speed compression profiles for this pulp. To do this, the curves of Fig. 7 have been converted to the original dimensional notation of the model and the results are presented in Fig. 9–11.

Fig. 9 shows the sulphite density profiles during the initial formation or acceleration period. Interpretation of the results must be qualified in view of assumptions (*2*) and (*7*), but, for depths greater than 10 μ (which is the mean order of fibre diameter in this case), the curves may be considered as a possible first approximation. They show the propagation of the mat face during formation and the compression from face to septum at given instants.

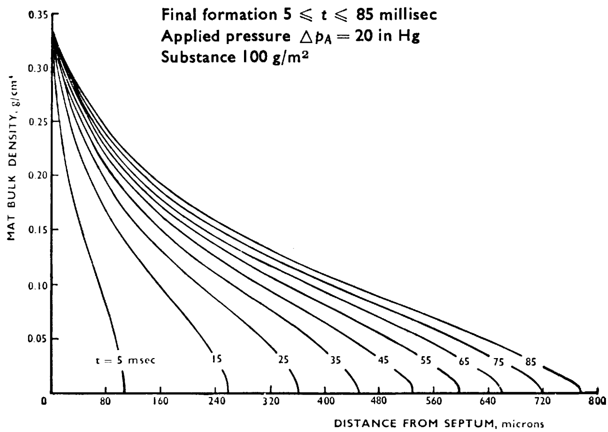

Fig. 10—Fibre mat density distribution $\rho_B(\chi, t')$—filtration of classified unbeaten sulphite fibres

As time increases, the relative compression rapidly increases until the density at the septum reaches the value corresponding to the total applied pressure. Compression characteristics during the constant pressure filtration are given in Fig. 10 up to final formation time, which is by definition the solution of—

$$L(t)-h(t) = 0 \quad . \quad . \quad . \quad . \quad (26)$$

and is 85 msec in this case.

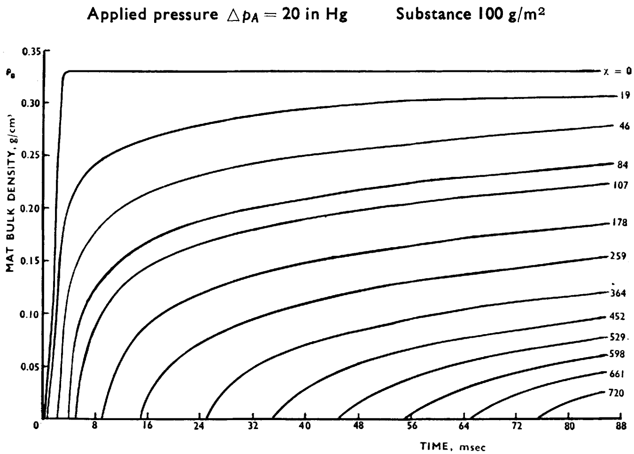

Fig. 11—Compression profiles in time $\rho_B(\chi, t)$—filtration of classified unbeaten sulphite fibres

Because a constant density is maintained at the septum, the density gradient decreases as the mat builds up in time. Fig. 11 contains the same information as Fig. 9 and 10, plotted to show the density profiles in time. At any of the indicated points above the septum, the actual pad density remains unspecified until such time as the pad depth overtakes the given distance, after which the density increases with time as shown. As expected, the most rapid increase is at the septum, where the equilibrium density is reached in the acceleration period. At all other points, the density continuously increases with time at rates depending on the distance concerned.

Results representing the flow rate distributions $R(\xi, t')$ have been obtained to correspond to each solution $\psi(\xi, t')$. The variation of flow rate with time at given relative depths within the mat was found in all cases to follow closely the pattern of the entrance speed $R_0(t')$. The partial change with respect to distance was at all times found to be very small, however, with the total variation from mat face to septum remaining less than 1 per cent. In certain cases, the effect of excluding assumption (*4*) was investigated and solutions were prepared to correct for fibre motion within the mat. The correction did not significantly change the result, consequently it is felt that the small increase in flow rate is due primarily to the very small pad depths and relatively low consistencies inherent in the parameter values investigated.

Experimental confirmation

To measure accurately the variables related by the theoretical compression curves presents a formidable problem in experimental technique, because of the low orders of magnitude involved. It is relatively much easier to study the motion of the suspension during high-speed mat formation. Since the slurry motion is theoretically dependent on the nature of the compression distributions, it may be considered that a direct confirmation of the former is additionally an indirect or partial corroboration of the latter.

The apparatus sketched in Fig. 1 has been used to study high-speed filtration. For this purpose, the mat depressor *f* is removed and the suspension is placed in chamber *B* to specified depth h_0. The technique is then similar to that described for permeation. During formation, filtration profiles $h(t)$ are recorded electronically with the aid of the depth probe *j*. The slurry speed is then obtained as a function of time by graphical differentiation of the profiles dh/dt.

Experiments were conducted at room temperature with a bleached sulphite fibre stock in the unbeaten state. Fines were removed with a Bauer-McNett classifier using No. 48 screen, which has a mesh slightly larger than the control screen of the apparatus. This ensured compatibility with assumptions

(*1*) and (*6*) of the theory. From independent laboratory tests on low-speed permeability and wet mat compression, the physical characteristics of this pulp were determined and are summarised as follows—

$$\left.\begin{aligned} S_0 &= 3.34\times 10^3\ \text{cm}^{-1} \\ \theta &= 1.81\ \text{cm}^3/\text{g} \\ m &= 1.37\times 10^7\ \text{c.g.s. units} \\ n &= 2.71 \end{aligned}\right| \quad . \quad . \quad . \quad (27)$$

Fibre suspensions at consistency 0.17 per cent were used to form a 100 g/m² sheet from initial depth $h_0 = 6$ cm at applied vacuums $\Delta p_A = 2$, 5 and 20 in Hg.

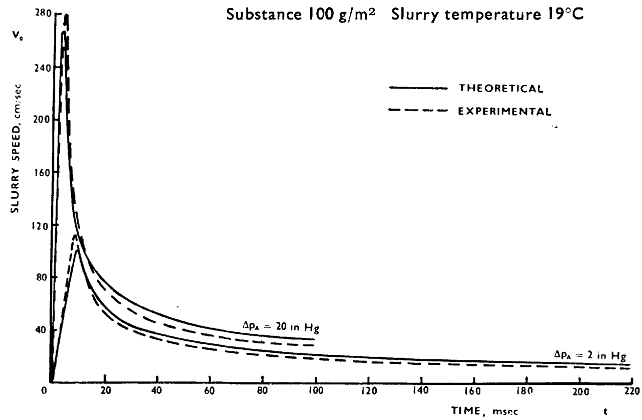

Fig. 12—Variation of slurry speed $V_0(t)$—filtration of classified unbeaten sulphite fibres

Results for the slurry motion $V_0(t)$ are shown in Fig. 12 for the low and high vacuums, having a standard deviation from the curve of ± 1.9 and ± 3.6 cm/sec, respectively. When the fibre mat characteristics given by equations (*27*) and these values of applied vacuum are used in equations (*21*), the fundamental parameters assume the values specified for the theoretical curves of Fig. 5. These theoretical curves have been replotted in dimensional form and are compared with the experimental results in Fig. 12. It is apparent that agreement is good, with the discrepancy almost within the experimental error. The theory predicts, however, a peak velocity that is slightly lower and final velocities higher than those observed.

The filtration profiles $h(t)$ may be obtained theoretically by the relationship—

$$h(t) = h_0 - \frac{mn\rho}{\theta^n \mu^2 S_0^3} \int_0^{t'} R_0(t')\, dt' \quad . \quad . \quad . \quad (28)$$

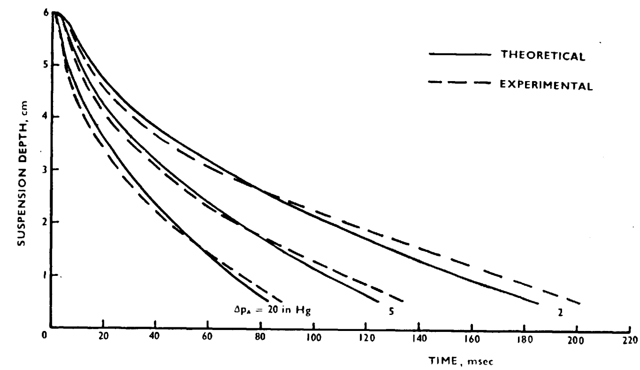

Fig. 13—Filtration profiles as a function of applied vacuum

which follows from the definition of h and R_0. The curves of Fig. 5 have been integrated according to equation (*28*) and the results are compared with the actual profiles in Fig. 13. Agreement may be considered satisfactory and the discrepancy in curvature is directly related to that of the corresponding rate curves in Fig. 12. It is evident from Fig. 13 that the theory has reasonably predicted formation times within 10 per cent of the observed values.

Similar calculations to determine the partial effect of the parameter β have yielded results for varying basis weight or consistency, shown dimensionally in Fig. 14. The experiments were performed at a constant applied vacuum, using consistencies necessary to produce the indicated basis weights. Since

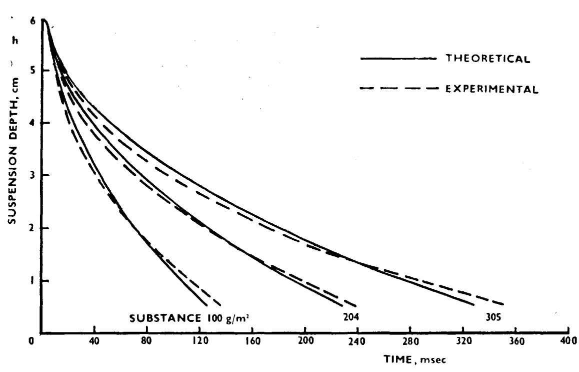

Fig. 14—Filtration profiles as a function of substance

the initial acceleration depends on the vacuum applied, the curves are identical at small times. Within the range investigated, the formation time appears to be approximately proportional to the basis weight. As before, prediction of the observations is reasonable, verifying that the theory represents a good first approximation.

Conclusions

HIGH-SPEED water permeation of fibre mats has been studied by correlating the pressure gradient developed across a mat with the fluid flow speed, density and viscosity, the mat porosity and fibre specific surface. The mathematical form of this correlation, equation (*4*), which has been taken from recent literature, was validated for an experimental range of specific surface 800–2 500 cm^{-1}, using uniform synthetic fibres packed at porosities 0.78–0.93 and using flow rates up to 180 cm/sec. With the aid of this expression and assuming its general applicability, a mathematical model of high-speed filtration has been investigated. Theoretical results with respect to the superficial kinematics of filtration have shown satisfactory agreement with direct measurements, thus confirming to some extent the predictions of mat formation and compression characteristics.

The calculations related to slurry motion have explained filtration in terms of three sequential processes—an initial uniform acceleration, a continuously increasing mat resistance causing deceleration and final formation with a constant pressure drop. The latter process is in practice usually the most significant, although the former two are nevertheless needed for reliable prediction of formation times and peak flow speed. It has been shown in addition that the more compressible media produce final filtration rates with the lowest sensitivity to applied pressure.

Theoretical estimates of the mat compression during filtration indicate that the more compressible materials may be characterised by a strong inflexion in the space density profiles, consequently giving rise to rapidly increasing density at the septum. Depending on compressibility, the rate at which the mat builds up decreases with increasing time after peak slurry velocity.

Analysis of the slurry motion has essentially explained the well-known facts related to the formation time under constant applied pressure. For the sulphite pulp studied, formation times vary with an inverse relation to pressure and are roughly proportional to the substance.

Acknowledgements

The author wishes to express his appreciation to Dr F. Lyth Hudson and Dr L. A. Kirk for valuable technical direction and discussion, as well as to the

Manchester College of Science and Technology, Department of Polymer and Fibre Science, for the provision of experimental facilities. Grateful acknowledgement is also given to the Departments of Computation and Computer Science for access to the Atlas digital computer of the University of Manchester.

The author is indebted to Peter Dixon & Son Ltd., who made the work possible through the award of the Joseph Dixon Fellowship.

References

1. Carman, P. C., *Flow of gases through porous media* (Butterworth Scientific Publication, London, 1956)
2. Prager, S., *The Physics of Fluids*, 1961, **4** (12), 1477–1482
3. Tiller, F. H. and Cooper, H. R., *A.I.Chem.E. J.*, 1960, **6** (4), 595–601
4. Ingmanson, W. L., *Tappi*, 1952, **35** (10), 439–448
5. Ingmanson, W. L. and Whitney, R. P., *Tappi*, 1954, **37** (11), 523–534
6. Whitney, R. P., Ingmanson, W. L. and Han, S. T., *Tappi*, 1955, **38** (3), 157–166
7. Ingmanson, W. L., Andrews, B. D. and Johnson, R. C., *Tappi*, 1959, **42** (10), 840–849
8. Meyer, H., *Tappi*, 1962, **45** (4), 296–310
9. Ergun, S., *Chem. Eng. Progr.*, 1952, **48** (2), 89–94
10. Ingmanson, W. L. and Andrews, B. D., *Tappi*, 1963, **46** (3), 150–155
11. Wahlström, B. and O'Blenes, G., *Pulp & Paper Mag. Can.*, 1962, **63** (8), T405–T417
12. Mardon, J., Truman, A. B., Howe, B. I. and Meadley, C. K., *Paper and Timber (Finland)*, 1961, **43** (8), 457–464; (9), 499–505; (10), 575–584, 586–588; (11), 681–695, 697–698
13. Meadley, C. K., *Can. J. Chem. Eng.*, 1962, **40** (6), 256–263; 1963, (3), 95–103
14. Meadley, C. K., to be published

Transcription of Discussion

Discussion

Chairman—There is sometimes a tendency to ask what is the relevance of this type of analytical study to the practical objective of making paper. I think it is important that we should attempt to answer this question. From an analytical viewpoint, the present-day Fourdrinier papermachine is a very complicated piece of equipment; I doubt very much whether we will ever work out the full hydrodynamics of it before it becomes obsolete. On the other hand, it is a very long step to translate or interpret some of the concepts developed in the laboratory, dealing with individual fibres and idealised networks, into relationships that can be of practical significance to our understanding and further development of the papermaking process.

I think this paper is a further step along a direction started in papers by W. L. Ingmanson, by H. Meyer and by R. W. Nelson, in which they have gradually put together some of these concepts of classical filtration, specific fibre surface and volume; put the compressibility of fibres and of fibre networks into a complete mathematical package; then gradually built up a body of experimental evidence to confirm that the concepts are sound.

In this latest paper, Meadley has considered very high-speed filtration and has included the effects of inertia forces. Once again, the emerging theory seems to hold up pretty well with the observed facts. This gives us, therefore, further confidence to apply theories based on the same assumptions to practical problems, even though we frequently find it necessary to introduce empirical factors to circumvent our present inability to achieve an exact mathematical solution for the complex situation of the practical case.

Dr J. A. Van den Akker—In my opinion, Meadley's paper understates the quality of agreement between theory and experiment. The importance of this excellent agreement is that it brings out the correctness of the underlying fundamental principles in drainage theory and indicates that, even after present papermachines are obsolete, these principles will apply to new processes involving filtration.

Chairman—I think that some of the current trends in the design of new papermachines will probably make our analytical problems easier in the future. Many of them are continuous forming devices with uniform or controlled suction zones.

Mr B. Radvan—Have you observed any effects of flocculation? From what we have heard (or are about to hear from Corte), if the drainage is by turbulent mechanism, then flocculation should have no effect on the speed of the drainage. This is certainly not true for slow machines; I have no experience of very fast machines.

I find Wahren's model of network—based on the concept of fibres straining against each other—very illuminating indeed: I am sure it is true. I am doubtful, however, of the argument that is advanced here to support it. Fig. 1 shows the decrease in the shear strength of the network when dispersed in a high viscosity medium: Perlon at 1.5 per cent. Unless these are very unusual fibres, I would expect them to be very flocculated in water; at high viscosities, they may very well be dispersed and there may be a simpler explanation.

Dr C. K. Meadley—In my experiments, I usually observe a certain amount of flocculation. The experiments were with synthetic fibre suspensions as well as with sulphite fibres and, commenting on Van den Akker's words, some of the results did not always compare with theory as well as the sulphite fibres did. It turned out that the sulphite results compared very well, because very dilute suspensions were used; but I had to go to higher consistencies with synthetic fibre suspensions in order to get a measurable pressure drop. This resulted in flocculation. The discrepancy between theory and experiment was of the same nature as that for sulphite fibres, but slightly greater and I actually explained this discrepancy in terms of flocculation. Therefore, I found much faster initial rates than I would have expected theoretically.

Dr D. Wahren—I would like to clarify a few points about Nissan's questions first. The motions in our apparatus are very small and slow. We are dealing with the same kind of thing as when testing solid materials. The question of boundary layer hydrodynamics, network breakdown and contraction of the network are therefore not applicable in this case. Actually, a network that is confined in a pipe, for instance, will tend to press against the walls. When slowly extruded into water, the network expands. The network pushes against the walls and is kept still by frictional forces, devèloped in the contact points by the normal forces. The exact nature of the frictional forces is probably of less importance in this case. The material in the elasto-viscometer cylinders is of very little importance. We get no difference in shear modulus when testing brass, stainless steel, plexiglass, paraffin and sandpaper, though we obtain some slight differences in shear strength and ultimate elongation. Of course, then we are dealing with large movements—of at least 1 mm.

Radvan's question prompts me to ask—which was first, the chicken or the egg? Using viscous media for dispersion of the fibre causes a drop in the network strength, owing to the inactivation of the fibres. Few fibres become active, because of the longer time available for the fibres to regain unstrained positions. On the other hand, the passive fibres will not flocculate, so a weaker network that is less flocculated results. The lack of flocculation is not the primary cause of the lower network strength or vice versa.